Transactions Papers

Minimum Mean-Squared Error Decision-Feedback Equalization for Digital Subscriber Line Transmission with Possibly Correlated Line Codes

David W. Lin, *Senior Member, IEEE*

Abstract— **Most of the published theory on the optimal performance of decision-feedback equalization under the MMSE criterion addresses the transmission of i.i.d. symbol sequences only. This paper presents a theory which accommodates the case of correlated symbol sequences. It also considers the use of a fractionally spaced forward filter in the decision-feedback equalizer (DFE). Two limiting conditions are discussed in some detail, both concerning having an infinite-length DFE feedback filter. In one of them the forward filter is of finite length and in the other it is noncausal infinite. Several numerical examples are given, in which we apply the theory to the study of the MMSE transmission performance, at ISDN basic access rates, of a few example subscriber lines using some well-known line codes. In these examples, the near–end crosstalk from identical digital transmission systems is assumed to be the only significant noise. Throughout the study, we ignore the effects of error propagation in a DFE.**

I. Introduction

Decision-feedback equalization for data transmission over dispersive channels has been a topic of continued study for some time [1]. Somewhat earlier applications include a high-rate coaxial transmission system [6] and a military tropospheric scatter radio system [7]. More recently, it has been used in digital subscriber line (DSL) terminals to support the ISDN (integrated services digital network) basic access over twisted-pair cables [8], [9]. Our interest here is in understanding its optimal performance, in the minimum mean-squared error (MMSE) sense, in the DSL environment.

Despite the amount of previous studies concerning decision-feedback equalization [1]–[5], we find the published theory unable to address our need fully. A major reason is that the published theory on MMSE equalization largely addresses the transmission of i.i.d. (independent and identically distributed) symbol sequences only, whereas in the area of DSL there has been a long standing interest in line coding schemes which yield non-i.i.d. outputs. More recently, Lechleider [11] augmented the theory to accommodate also the case of correlated symbol sequences. The present author [12] also reported a study which not only considered correlated symbol sequences, but also allowed for a fractionally spaced forward filter in the DFE (decision-feedback equalizer). However, these publications are concerned with finite-length DFE's only. McGee [10] considered infinite-length DFE's in correlated symbol sequences. However, he assumed their analog front-ends to be optimal, a common assumption which in practice can only be approximated at best and one which we do not make in this study. Further, the extension of his results to the conditions we are interested in is not an obvious matter.

The performance of an infinite-length DFE is of interest although practical DFE's are always of finite lengths. This is because it provides information on the limit of MMSE equalization and can serve as a benchmark against which the performance of a finite-length DFE may be compared. To some extent, we can liken its role to that played by the channel capacity in the design of communications systems. Now, the input to the feedback filter is a digital signal with only a very limited number of levels, while that to the forward filter is continuous in amplitude. Hence it is more difficult to implement a long forward filter than a long feedback filter, due to the amount of multiplication required with the former. Thus, for the sake of benchmarking at least, it is of interest to study the performance of MMSE decision-feedback equalization in the limit of an infinite-length feedback filter, while holding finite the length of the forward filter. This limiting case is addressed in this paper, as well as that of having an infinite-length feedback filter with an infinite-length forward filter, both in the situation of correlated symbol sequences.

In summary, therefore, the aim of this paper is twofold. First, to present a theory on MMSE equalization for DFE's (especially infinite-length ones) operating in correlated symbol sequences; and second, to illustrate their performance in the DSL environment by way of some numerical examples.

Schematically, the equalization problem considered can be pictured as in Fig. 1(a) where the "channel" includes all analog transmission filtering, as depicted in Fig. 1(b) for the case of DSL transmission. (Hybrids are transformer circuits for coupling transceivers with the transmission line. An example will be shown later.) For generality, the DFE forward filter

Paper approved by the Editor for Channel Equalization of the IEEE Communications Society. Manuscript received February 6, 1989; revised November 15, 1989 and March 29, 1990.

The author is with the Department of Electronics Engineering and the Center for Telecommunications Research, National Chiao Tung University, Hsinchu Taiwan 30050, ROC, on leave from Bellcore, Red Bank, NJ 07701.

IEEE Log Number 9100820.

0090–6778/91/0800–1197$01.00

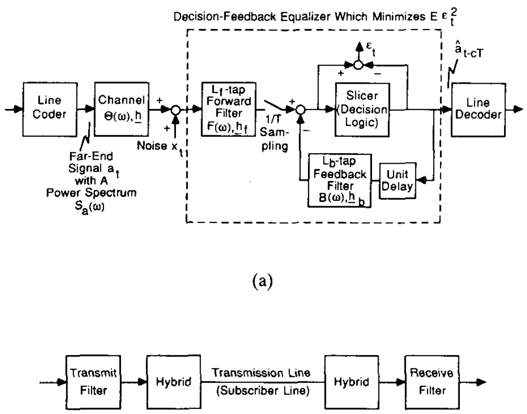

(a)

(b)

Fig. 1. The MMSE equalization problem. (a) Problem frame work. (b) Details of the channel.

is assumed to be possibly fractionally spaced with a temporal tap spacing kT/m where T is the symbol period and k and m are coprime integers with $k \leq m$, including the case $k = m = 1$. In Fig. 1(a), $\underline{h}$ denotes the vector of channel impulse response sampled at T/m spacing and Θ the corresponding frequency response, i.e., $\Theta(\omega) = \sum_{i=0}^{\infty} h_i e^{-ji\omega T/m}$ where we have let $\underline{h} = [h_0, h_1 h_2, \cdots]'$, with $'$ denoting matrix transpose. The noise x is also assumed to be sampled at T/m spacing. The vectors $\underline{h}_f$ and $\underline{h}_b$ represent, respectively, the impulse responses of the kT/m-spaced DFE forward filter and the T-spaced DFE feedback filter, while F and B the corresponding frequency responses. We have also assumed an overall transmission delay (cursor delay) of c symbol periods. Note from Fig. 1(a) that, unlike in some earlier studies [2]–[5], [10], we do not consider the analog front-end as part of the DFE. In other words, we assume the response of the analog front-end to be fixed and not optimizable. This is because analog filters are less easily made adaptive to minimize the MSE (mean-squared error) as shown.

In the following, Section II outlines a general solution to the MMSE decision-feedback equalization problem. It serves to establish some notions for later use. Section III then develops the results to address the case of an infinite-length feedback filter with a finite-length forward filter, and Section IV the case where both the forward and the feedback filters are infinite in length. Section V applies the theory to a few example subscriber lines to investigate their transmission performance under MMSE decision-feedback equalization. Section VI concludes the paper. In this work, the problem of error propagation in DFE's is not addressed.

II. MMSE Decision-Feedback Equalization

As often done, we assume that the slicer in the DFE makes no incorrect decisions, which should be approximately true during normal operation at a low error rate. Then the transmission path is mathematically equivalent to the one shown in Fig. 2. Assume further that the signal and the noise are uncorrelated with each other. Then, by examining

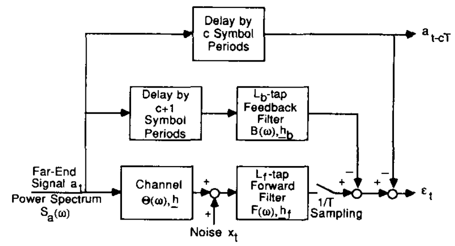

Fig. 2. A mathematically equivalent problem when the DFE slicer makes no decision error.

Fig. 2, we can write down an expression for the mean-squared decision-point error. For this, note first that the combined impulse response of the channel and the DFE forward filter is, after T-spaced sampling, given by $\boldsymbol{M'HK}\underline{h}_f$ where $\boldsymbol{H}$ is a lower triangular Toeplitz matrix having h as its first column (padded with trailing zeros as needed), $\boldsymbol{K}$ is an L_f-column matrix whose ik + 1st column is the ik + 1st column of the identity matrix ($i = 0, 1, 2, \cdots, L_f - 1$), and $\boldsymbol{M}$ is a matrix whose ik + 1st column is the im + 1st column of the identity matrix ($i = 0, 1, 2, \cdots$) [12]. The MSE is thus given by (assuming a certain given cursor delay c)

$$E\{\varepsilon_{iT}^2 | \underline{h}_f, \underline{h}_b\} = E\{[(\boldsymbol{M'HK}\underline{h}_f - \boldsymbol{P}\underline{h}_b - \underline{e}_c)' \cdot \underline{a}_{iT} + \underline{h}_f'\boldsymbol{K}'\underline{x}_{iT}]^2\}$$
$$= (\boldsymbol{M'HK}\underline{h}_f - \boldsymbol{P}\underline{h}_b - \underline{e}_c)'\boldsymbol{R}_a \cdot (\boldsymbol{M'HK}\underline{h}_f - \boldsymbol{P}\underline{h}_b - \underline{e}_c) + \underline{h}_f'\boldsymbol{K}'\boldsymbol{R}_x\boldsymbol{K}\underline{h}_f \quad (1)$$

where E denotes expectation; $\underline{a}_{iT}$ and $\underline{x}_{iT}$ are, respectively, vectors of far-end signal symbols and noise samples, arranged in reverse time order and led by a_{iT} and x_{iT}, respectively, $\boldsymbol{R}_a$ and $\boldsymbol{R}_x$ are the corresponding autocorrelation matrices; $\underline{e}_c$ is the c + 1st column of the identity matrix; and $\boldsymbol{P}$ is a matrix composed of the c + 2nd through the $c + L_b$ + 1st columns of the identity matrix.

All of the vectors and matrices in (1) can be of infinite dimension. Also, note that $\boldsymbol{M'HK}$ is basically block Toeplitz with $k \times m$-sized blocks. Further, if the channel noise is dominated by self-NEXT (*n*ear-*e*nd *cross*talk from identical DSL systems), then, by the T/m-spaced sampling of x, the matrix $\boldsymbol{R}_x$ is either Toeplitz or block-Toeplitz with $m \times m$-sized blocks; and so is $\boldsymbol{K'R_xK}$.

Minimization of the MSE involves a straightforward exercise of the least-squares technique [12], which yields the following MMSE DFE:

$$\underline{h}_f^{\text{opt}} = \boldsymbol{R}_1^{-1}\rho_1, \quad (2a)$$

$$\underline{h}_b^{\text{opt}} = (\boldsymbol{P'R_aP})^{-1}\boldsymbol{P'R_a}(\boldsymbol{M'HK}\underline{h}_f^{\text{opt}} - \underline{e}_c), \quad (2b)$$

and the following MMSE:

$$\sigma_\varepsilon^2 \equiv \min_{\underline{h}_f, \underline{h}_b} E\{\varepsilon_{iT}^2 | \underline{h}_f, \underline{h}_b\}$$
$$= \sigma_a^2 - \underline{e}_c'\boldsymbol{R}_a\boldsymbol{P}(\boldsymbol{P'R_aP})^{-1}\boldsymbol{P'R_a}\underline{e}_c - \underline{\rho}_1'\boldsymbol{R}_1^{-1}\rho_1, \quad (3)$$

where

$$\boldsymbol{R}_1 = \boldsymbol{K}'\boldsymbol{R}_x\boldsymbol{K} + \boldsymbol{K}'\boldsymbol{H}'\boldsymbol{M} \cdot [\boldsymbol{R}_a - \boldsymbol{R}_a\boldsymbol{P}(\boldsymbol{P}'\boldsymbol{R}_a\boldsymbol{P})^{-1}\boldsymbol{P}'\boldsymbol{R}_a]\boldsymbol{M}'\boldsymbol{H}\boldsymbol{K}, \quad (4a)$$

$$\underline{\rho}_1 = \boldsymbol{K}'\boldsymbol{H}'\boldsymbol{M}[\boldsymbol{R}_a - \boldsymbol{R}_a\boldsymbol{P}(\boldsymbol{P}'\boldsymbol{R}_a\boldsymbol{P})^{-1}\boldsymbol{P}'\boldsymbol{R}_a]\underline{e}_c, \quad (4b)$$

and

$$\sigma_a^2 = \underline{e}_c'\boldsymbol{R}_a\underline{e}_c \quad (4c)$$

(i.e., the far-end signal power). In writing (2)–(4), we have assumed the invertibility of $\boldsymbol{R}_1$ and $\boldsymbol{P}'\boldsymbol{R}_a\boldsymbol{P}$ which can be shown to hold for finite-length DFE's. The invertibility may be a concern for infinite-length DFE's and it will be addressed in later sections. Also, note that (2)–(4) simplify significantly when we have uncorrelated symbol sequences, i.e., when $\boldsymbol{R}_a = \sigma_a^2\boldsymbol{I}$. (For simplicity, we shall use the same notation $\boldsymbol{I}$ to denote identity matrices of different dimensions, when confusion is unlikely.)

After equalization, the nominal SNR (signal-to-noise ratio) is given by $\sigma_a^2/\sigma_\varepsilon^2$. It can be used to measure the transmission performance, subject to the concerns discussed in [12], such as the possible signal-dependence of noise variance. For notational simplicity, hereafter we omit the superscript *opt* from $\underline{h}_f^{\text{opt}}$ and $\underline{h}_b^{\text{opt}}$, because all subsequent references to $\underline{h}_f$ and $\underline{h}_b$ are to their MMSE values.

III. DFE with an Infinite-Length Feedback Filter and a Finite-Length Forward Filter

To apply the MMSE solution to the case of an infinite-length DFE feedback filter, note first that the matrix $\boldsymbol{P}$ in this case is semi-infinite and so is $\boldsymbol{P}'\boldsymbol{R}_a\boldsymbol{P}$. By the Toeplitz nature of $\boldsymbol{R}_a$, we have $\boldsymbol{P}'\boldsymbol{R}_a\boldsymbol{P} = \boldsymbol{R}_a$. It is trivial to invert $\boldsymbol{R}_a$ when it is diagonal. For many line codes, however, it is not only nondiagonal but also singular because of the deliberately designed spectral zeros on the unit circle [14]. Examples of such codes are the precoded dicode (or bipolar, or AMI) [15], the precoded MDB (*m*odified *d*uobinary, or class-4 partial-response) [15], and the MS43 [16], [17] codes. For them the use of inverse of $\boldsymbol{P}'\boldsymbol{R}_a\boldsymbol{P}$ in the MMSE solution has to be reexamined. In MMSE estimation with a finite-length estimator, a convenient tool to handle this kind of problem is the generalized matrix inverse [18], [19]. It turns out that, in our case, we can also define a special kind of matrix inverse for $\boldsymbol{R}_a$ to make valid the solution as formulated in (2)–(4). This inverse can be described in terms of a spectral factorization [20], [2] of $S_a(\omega)$, the power spectrum of the far-end signal.

To this end, let $\{v_i\}$ be a zero-mean Gaussian random sequence whose power spectrum is equal to $S_a(\omega)$ also. Then $\{v_i\}$ can be represented as a causal moving average of a white sequence $\{u_i\}$ as $v_i = u_i + p_1u_{i-1} + p_2u_{i-2} + \cdots$. The sequences $\{u_i\}$ and $\{p_i\}$ are related to $S_a(\omega)$ as

$$S_a(\omega) = \sigma_u^2|P(\omega)|^2 \quad (5)$$

where σ_u^2 denotes the variance of u_i and $P(\omega) = \sum_{i=0}^{\infty} p_i e^{-ji\omega T}$, with $p_0 \equiv 1$. In other words, σ_u^2 and $P(\omega)$ denote a spectral factorization of $S_a(\omega)$. It is not hard to show that

$$\boldsymbol{R}_a = \sigma_u^2\Pi'\Pi \quad (6)$$

where Π is a lower triangular Toeplitz matrix whose first column is given by $[1, p_1, p_2, \cdots]'$. Now, let $\{1, q_1, q_2, \cdots\}$ be the causal inverse of $\{1, p_1, p_2, \cdots\}$, i.e., $Q(\omega) \equiv \sum_{i=0}^{\infty} q_i e^{-ji\omega T} = \frac{1}{P(\omega)}$, with $q_0 \equiv 1$. (The system $Q(\omega)$ is marginally stable when $S_a(\omega)$ contains spectral zeros.) The sequence $\{-q_1, -q_2, \cdots\}$, in fact, gives the infinite-order one-step linear MMSE predictor for the process $\{v_i\}$ and σ_u^2 is equal to the variance of the infinite-order one-step prediction error. We are now ready to define the special kind of inverse for $\boldsymbol{R}_a$, denoted $\boldsymbol{R}_a^\dagger$:

$$\boldsymbol{R}_a^\dagger \equiv \frac{1}{\sigma_u^2}\Psi\Psi' \quad (7)$$

where Ψ is a lower triangular Toeplitz matrix with its first column given by $[1, q_1, q_2, \cdots]'$. Proof that the use of this inverse in (2)–(4) does result in the desired MMSE solution for the problem will be omitted here. Simply put, it involves a verification of the equivalence of the range subspaces of some singular linear transformations, much the same as in the case of generalized matrix inverses.

The evaluation of σ_u^2 and p_i for the various line codes is not a difficult task. For a partial-response code, $\{p_i\}$ is simply given by the partial-response filter and σ_u^2 the power of filter input. For a block code, its power spectrum is a finite-order rational function in the Z-transform domain and can be calculated by an established method [17]. The spectral factorization can thus be done by factoring the numerator and the denominator of that function, followed by a long division. As a numerical example, Table I gives the power spectrum of the MS43 code and its spectral factorization.

To calculate the MMSE solution as given in (2)–(4), then, we note that, by (6) and (7),

$$\boldsymbol{R}_a - \boldsymbol{R}_a\boldsymbol{P}(\boldsymbol{P}'\boldsymbol{R}_a\boldsymbol{P})^\dagger\boldsymbol{P}'\boldsymbol{R}_a = \sigma_u^2\Pi'(\boldsymbol{I} - \boldsymbol{P}\boldsymbol{P}')\Pi \quad (8)$$

which is everywhere zero except for the leading $(c+1) \times (c+1)$ submatrix. In fact, this matrix can be interpreted as the autocorrelation of error in estimating the infinite vector $[v_i, v_{i-1}, v_{1-2}, \cdots]'$ from $\{v_{i-c-1}, v_{i-c-2}, \cdots\}$ by a linear (matrix) MMSE estimator. The quantity of $\sigma_a^2 - e_c'\boldsymbol{R}_a\boldsymbol{P}(\boldsymbol{P}'\boldsymbol{R}_a\boldsymbol{P})^\dagger\boldsymbol{P}'\boldsymbol{R}_a\underline{e}_c$ appearing in (3) is simply the c + 1st diagonal element of the above matrix and is equal to σ_u^2. (These results can also be derived using the notion of innovations [20].) Therefore, the MMSE can be expressed as

$$\sigma_\varepsilon^2 = \sigma_u^2 - \underline{\rho}_1'\boldsymbol{R}_1^{-1}\underline{\rho}_1 \quad (9a)$$

where

$$\boldsymbol{R}_1 = \boldsymbol{K}'\boldsymbol{R}_x\boldsymbol{K} + \sigma_u^2\boldsymbol{K}'\boldsymbol{H}'\boldsymbol{M}\Pi'(\boldsymbol{I} - \boldsymbol{P}\boldsymbol{P}')\Pi\boldsymbol{M}'\boldsymbol{H}\boldsymbol{K} \quad (9b)$$

and

$$\underline{\rho}_1 = \sigma_u^2\boldsymbol{K}'\boldsymbol{H}'\boldsymbol{M}\Pi'(\boldsymbol{I} - \boldsymbol{P}\boldsymbol{P}')\Pi_{\underline{e}_c} = \sigma_u^2\boldsymbol{K}'\boldsymbol{H}'\boldsymbol{M}\Pi'\underline{e}_c. \quad (9c)$$

TABLE I
POWER SPECTRUM OF THE MS43 CODE AND ITS SPECTRAL FACTORIZATION

	Power Spectrum
Denominator =	$22.4 \cdot [(z^6 + z^{-6}) + 9.225(z^3 + z^{-3}) - 29.2390625]$
Numerator =	$-(z^8 + z^{-8}) - 6.8(z^7 + z^{-7}) + 69(z^6 + z^{-6}) - 17.465(z^5 + z^{-5}) - 70.66(z^4 + z^{-4})$ $+ 592.425(z^3 + z^{-3}) + 14.6075(z^2 + z^{-2}) + 292.255(z^1 + z^{-1}) - 1744.725$
	Spectral Factorization
Error Variance =	2.1944
Denominator =	$1 - 0.375z^{-3} - 0.0390625z^{-6}$
Numerator =	$1 - 0.34952z^{-1} - 0.16995z^{-2} - 0.47986z^{-3} + 0.048764z^{-4}$ $- 0.0031980z^{-5} - 0.052713z^{-6} + 0.0056816z^{-7} + 0.00079469z^{-8}$
Series Expansion =	$1 - 0.34952z^{-1} - 0.16995z^{-2} - 0.10486z^{-3} - 0.082306z^{-4}$ $- 0.066928z^{-5} - 0.052974z^{-6} - 0.038836z^{-7} - 0.030942z^{-8}$ $- 0.023961z^{-9} - 0.017779z^{-10} - 0.014218z^{-11} - 0.011055z^{-12}$ $- 0.0081840z^{-13} - 0.0065403z^{-14} - 0.0050815z^{-15} - 0.0037635z^{-16}$ $- 0.0030080z^{-17} - 0.0023374z^{-18} - 0.0017310z^{-19} - 0.0013835z^{-20}$ $+ \cdots$

The optimal DFE forward filter is again given by $\underline{h}_f = \boldsymbol{R}_1^{-1}\underline{\rho}_1$. The optimal DFE feedback filter can be shown by using (6) and (7) in (2b) to be

$$\underline{h}_b = \Psi \boldsymbol{P}'\Pi(\boldsymbol{M}'\boldsymbol{H}\boldsymbol{K}\underline{h}_f - \underline{e}_c). \tag{10}$$

By the Toeplitz nature of Π and Ψ, multiplications with them can be viewed as convolutions and carried out in the frequency domain by multiplying with $P(\omega)$ and $Q(\omega)$. The possible existence of unit-circle poles in $Q(\omega)$, due to the spectral zeros of $S_a(\omega)$, causes no stability problem because these poles are canceled by the corresponding zeros of $P(\omega)$.

IV. DFE WITH BOTH FILTERS INFINITE IN LENGTH

We now consider a DFE whose forward and feedback filters are both infinite in length. As mentioned, this DFE structure has been studied in various contexts short of what we are interested in [2], [4], [10]. And the extension of these previous results to our situation is not an obvious matter.

As in the earlier studies, we assume the forward filter to be noncausal, i.e., infinite in both directions of time, while the feedback filter strictly causal and semi-infinite. In terms of our time-domain formulation given in the previous sections, this DFE structure can be considered as first letting the cursor delay $c \to \infty$, letting the forward-filter length $L_f = 2cm/k \to \infty$, and then shifting the time origin to where the cursor is. After the shift of time origin, the cursor delay becomes zero relative to the new "time zero" and the forward filter becomes noncausal and two-sided infinite.

Due to its length and mathematical nature, we leave the derivation of the MMSE solution to the Appendix. Below we summarize the results for the situation where $k = 1$, assuming that the sampled noise process x is stationary and letting $S_x(\omega)$ denote its power spectrum. In this situation, the MMSE forward filter is given by, in the frequency domain,

$$F(\omega) = \frac{\sigma_u^2\sigma_\gamma^2\Theta^*(\omega)P^*(\omega)\gamma^*(\omega)}{S_x(\omega)} \tag{11}$$

where * denotes complex conjugation, σ_u^2 and $P(\omega)$ are defined in the last section, and σ_γ^2 and $\gamma(\omega)$ define a spectral factorization of $1 + S_a(\omega) \cdot \frac{1}{m}\sum_{i=0}^{m-1}\frac{|\Theta(\omega_i)|^2}{S_x(\omega_i)}$ (where $\omega_i = \omega + \frac{2\pi i}{T}$) in the sense that

$$1 + S_a(\omega) \cdot \frac{1}{m}\sum_{i=0}^{m-1}\frac{|\Theta(\omega_i)|^2}{S_x(\omega_i)} = \frac{1}{\sigma_\gamma^2|\gamma(\omega)|^2} \equiv A(\omega). \tag{12}$$

The MMSE feedback filter is given by

$$B(\omega) = e^{j\omega T}\left[\frac{1}{P(\omega)\gamma(\omega)} - 1\right]. \tag{13}$$

And the MMSE is simply

$$\sigma_\varepsilon^2 = \sigma_u^2\sigma_\gamma^2. \tag{14}$$

A comparison of (11) with the earlier results concerning i.i.d. symbol sequences, such as those in [4], reveals that the difference lies mainly in the presence of σ_u^2 and $P(\omega)$. In fact, the factor $\frac{\Theta^*(\omega)P^*(\omega)}{S_x(\omega)}$ in (11) corresponds to the matched-filter front-end of the conventional MMSE DFE[4]. Note also that neither $P(\omega)$ nor $\gamma(\omega)$ is needed in calculating the MMSE σ_ε^2 and hence the nominal SNR $\sigma_a^2/\sigma_\varepsilon^2$, but only σ_u^2 and σ_γ^2; of which the latter can be evaluated from $A(\omega)$ using the well-known equality that [21], [22], [2]

$$\sigma_\gamma^2 = \exp\left[-\frac{T}{2\pi}\int_0^{\frac{2\pi}{T}} \ln A(\omega)\, d\omega\right] \tag{15}$$

and the former from $S_a(\omega)$ by the technique of rational-function factorization described earlier.

Interestingly, a simple expression exists for each of the two constituents of the MMSE, viz., the filtered channel-noise power and the equalization error power. The former is given by $\underline{h}_f'\boldsymbol{K}'\boldsymbol{R}_x\boldsymbol{K}\underline{h}_f$ and the latter $\sigma_\varepsilon^2 - \underline{h}_f'\boldsymbol{K}'\boldsymbol{R}_x\boldsymbol{K}\underline{h}_f$. By (A.10),

$$\underline{h}_f'\boldsymbol{K}'\boldsymbol{R}_x\boldsymbol{K}\underline{h}_f = \sigma_\varepsilon^2\left[1 - \frac{T}{2\pi}\int_0^{\frac{2\pi}{T}}\frac{1}{A(\omega)}d\omega\right]. \tag{16}$$

TABLE II
SYMBOL ERROR RATE VS. REQUIRED SNR (IN DB) FOR SOME LINE CODES IN TRANSMISSION OVER A GAUSSIAN NOISE CHANNEL

Line Code → ↓ Error Rate	(N)RZ	Precoded Dicode, Precoded MDB	MS43	3B2T	2B1Q
10^{-6}	13.5	16.7	17.8	18.4	20.7
10^{-7}	14.3	17.5	18.5	19.2	21.4
10^{-8}	15.0	18.1	19.2	19.8	22.1

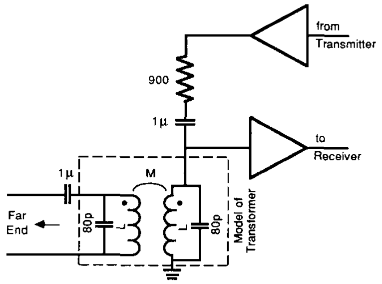

Fig. 3. An example hybrid network.

V. NUMERICAL EXAMPLES

As examples, we consider the DFE performance on the six loops (subscriber lines) used in a previous study [13]. As in [13], we also consider two simple 26-gauge PIC (polyethylene-insulated cable) lines of lengths 2.5 and 3 miles, respectively, for a comparison. Although we shall sometimes refer to this effort as a simulation, we do not mean a "real" simulation done in a sample by sample fashion. Instead, the above-developed theory is used to calculate the numerical results.

We consider the following six line codes: (N)RZ ([*n*on-] *r*eturn-to-*z*ero – coding 1 as +1 and 0 as −1; waveform returns or does not return to zero depending on the duty cycle) [24], dicode (precoded), MDB (precoded), MS43, 3B2T (3 *b*inary-to-2 *t*ernary, excluding 00), and 2B1Q (2 *b*inary-to-1 *q*uaternary). Table II lists the required SNR for symbol detection in signal-independent additive Gaussian noise for these codes at several symbol error rates. (This table is more accurate than Table I of [12].) We let the bit rate be that considered for the ISDN basic access, i.e., 160 kb/s, except in the case of the 3B2T code where for divisibility by three we let the bit rate be 162 kb/s.

The simulated hybrid network has the configuration shown in Fig. 3 where the $1\mu F$ capacitors are for DC blockage. Interestingly, we have found the 900 Ω resistance to result in a better SNR performance than the 135 Ω used in some studies, although the latter is closer in value to the characteristic impedance of the lines at the considered frequencies. This could be due to the combined effect of various factors which we do not intend to analyze here. The transformer windings are assumed to be perfectly coupled so that $M = L$. Two values of L are considered, namely, $L = 40$ mH and $L = 3.5$ mH. (This hybrid network only serves as an example and is in no way claimed to be the best design. Same is true for the transmission filters to be described later.)

The impulse responses of the loops have been calculated as described in [13]. As in [13], we have assumed their frequency responses to be negligible beyond twice the baudrate in each case—equivalent to assuming brickwall low-pass filtering with a cutoff at twice the baudrate. Because of this we have not included an antialiasing low-pass filter in the simulated transceiver. The combined characteristics of the transmit and the receive filters are the same as the 21–tap FIR filter described in [13], in series with a first-order analog high-pass filter. Data symbols are transmitted with a 25% duty cycle because the FIR filter operates at 4 times the baudrate. We let the corner frequency of the first-order analog high-pass filter be variable with the line code and the DFE length. For each line code and each DFE length, it is determined by choosing from a set of frequencies the one yielding a better SNR, where the set consists of seven frequencies at, respectively, 0, 0.025, 0.05, 0.1, 0.15, 0.2, and 0.25 times the baudrate. (A corner frequency at 0 means a flat unity gain, i.e., no high-pass filtering.) It happens that this chosen frequency has been zero in all the examples presented below.

The noise is assumed to be dominated by self-NEXT which is known to have a power transfer function $Kf^{3/2}$ where f is the frequency in Hz and K is a parameter depending on the crosstalk strength [25]. Further, we assume that the composite self-NEXT noise is stationary (instead of merely cyclostationary as the digital waveform in each individual crosstalking system is). Also for simplicity, we arbitrarily assume that the crosstalkers consist solely of 2 mile 26 gauge PIC lines. (The results from assuming 2 mile 26 gauge crosstalkers composed of pulp-insulated lines differ from those obtained under the above assumption by less and 0.1 dB in all examples below.) We let $K = 10^{-13}$, which corresponds roughly to the 49 crosstalker curve in [26]. (The data presented in [26] were obtained through computer simulation of crosstalk in 18 kft 22 gauge PIC lines which were terminated in their characteristic impedance. Although this condition is different from ours, we should have been conservative by using its data, at least for the two reasons below. First, 26 gauge lines incur more loss per unit length than 22 gauge ones and hence the crosstalk power will probably be lower on the average. And second, the data in [26] are for severe NEXT disturbance which has only 1% cumulative probability of occurrence.)

Consider now the situation of a DFE having a noncausal infinite-length $T/2$-spaced forward filter and a semi-infinite feedback filter. For it we obtain a better result with $L = 40$ mH than with $L = 3.5$ mH. Fig. 4 shows the result from having $L = 40$ mH where for ease of comparison we have normalized the SNR values with respect to that required for a 10^{-7} symbol error rate. In other words, we have subtracted 14.3, 17.5, 18.5 dB, etc., from the performance of the (N)RZ, the pre-

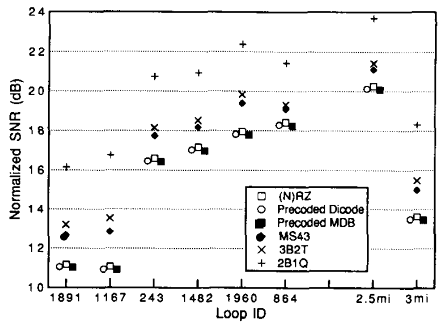

Fig. 4. Transmission performance (subscriber to central office) with an MMSE DFE having an infinite $T/2$-spaced forward filter and a semi-infinite feedback filter.

coded dicode, the MS43, etc., respectively; so that, if the decision-point error ε is Gaussian and signal-independent, than a 0 dB normalized SNR corresponds to a 10^{-7} symbol error rate. We have also included a very small amount of band-limited white noise in x to avoid the need to handle division by zero in the computation of $A(\omega)$ which would otherwise arise sometimes. This should not have caused appreciable difference in the result. In obtaining the result, we have also otimized the receiver's timing by considering 16 equispaced candidate sampling phases and picking the one yielding the minimum MMSE. As seen, in Fig. 4 we have ordered the six loops according to ascending SNR performance.

Interestingly, the MMSE performance obtained using a T-spaced forward filter is effectively the same as that using a $T/2$-spaced: the difference being less than 0.1 dB in all code and loop combinations. With a moderately suboptimal timing phase ($\pm 1/16$ of a symbol interval away from the optimal), the performance of the $T/2$-spaced equalizer stays intact, and that of the T-spaced suffers little (less than 0.1 dB in all cases), too. The performance difference becomes more conspicuous with a more suboptimal timing phase, however. For the T-spaced equalizer, a $\pm 1/4$ symbol interval's phase offset from the optimal leads to a performance degradation of up to about 0.85 dB and a $\pm 1/2$ symbol interval's offset one of up to 2.7 dB; while for the $T/2$-spaced equalizer, less than 0.05 dB of maximum degradation is caused in these situations. This echoes the frequently observed result that fractionally spaced equalizers suffer less from timing suboptimality than synchronous ones in diverse situations in a different context.

We now shorten the forward filter to finite lengths but keep the length of the feeback-filter infinite. Fig. 5 depicts some results, again with $L = 40$ mH because it yields a better performance. The forward filters are again $T/2$-spaced. The decision delay has again been optimized up to $1/16$ of a symbol period in each case. Fig. 6(a) plots the reduction in MMSE SNR from using an infinite-length forward filter to using an 8–tap one, and Fig. 6(b) that from using an 8–tap forward filter to using a 3–tap one. It is interesting that the SNR reduction for each code is quite even across the different loops in either situation.

As may be expected, timing suboptimality now exerts a greater influence on the equalizer's SNR performance for these shorter forward-filter lengths than for a length of infinity. With a $\pm 1/16$ symbol interval's phase offset, a worst case SNR degradation of 0.6 dB (among all code and loop combinations)

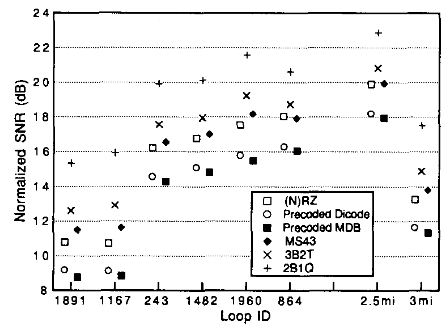

(a)

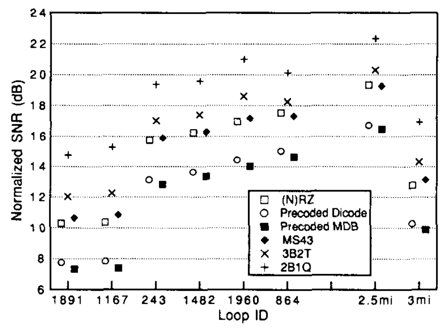

(b)

Fig. 5. Transmission performance (subscriber to central office) with an MMSE DFE whose feedback filter is semi-infinite in length and whose forward filter is $T/2$-spaced. (a) Length of forward filter = 8. (b) Length of forward filter = 3.

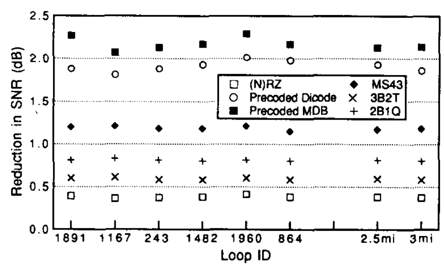

(a)

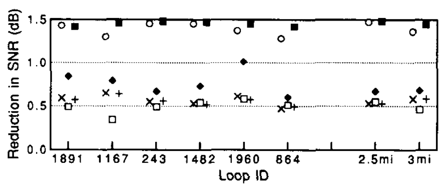

(b)

Fig. 6. Reduction in transmission performance from shortening the DFE forward filter. Feedback filter is semi-infinite in length. (a) As forward filter is shortened from of infinite length to 8 taps. (b) As forward filter is shortened from 8 taps to 3 taps.

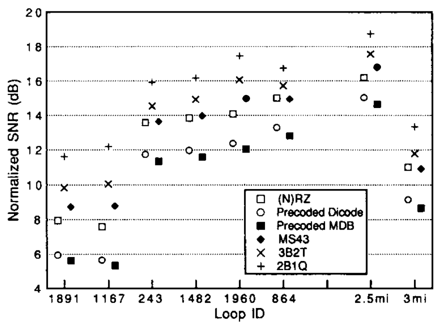

(a)

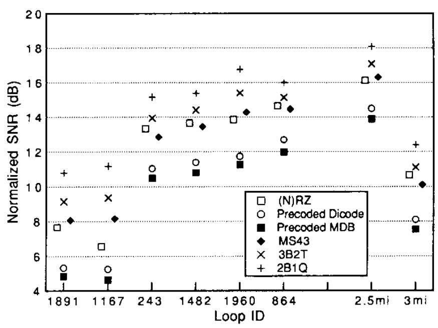

(b)

Fig. 7. Transmission performance (subscriber to central office) with an MMSE DFE whose feedback filter is 30-tap long. Forward filter is $T/2$-spaced. (a) Length of forward filter = 8. (b) Length of forward filter = 3.

is found in the 8–tap situation, and one of 2.0 dB in the 3–tap situation.

Finally, let us shorten the feedback filter length to 30 taps while keeping the forward-filter lengths at 8 and 3 taps. This time we get a better performance with $L = 3.5$ mH. The corresponding result from using optimal decision delays is shown in Fig. 7. Fig. 8(a) plots the SNR reduction from having an infinite-length feedback filter to having a 30 tap one, at a forward filter length of 8 taps; and Fig. 8(b) that from having an 8 tap forward filter to having a 3 tap one, at a feedback-filter length of 30 taps. On the effect of suboptimal timing, we find a worst case degradation of 0.65 dB among all code and loop combinations in the situation of an 8 tap forward filter, and one of 2.25 dB in the situation of a 3 tap forward filter, again at a $\pm 1/16$ symbol interval's offset from the optimal delay. It is likely that timing suboptimality will cause a worse degradation if we further shorten the feedback filter [27].

It is interesting to note that, in all these examples, the transmission performance is reversely related to the baudrate, except in the case of the simple (N)RZ, which often performs as well as the MS43.

VI. Conclusion

We presented a theory on MMSE decision-feedback equalization which augments previously published results by allowing both a correlated symbol sequence and a fractionally spaced DFE forward filter. This theory facilitates our calculating the potential DSL transmission performance in cases of correlated line codes, especially for situations where one or both of the DFE filters are infinite in length. The situation of an infinite-length DFE is of interest because it provides information on the limit of MMSE equalization and can thus serve as a benchmark against which the performance of a finite-length DFE may be compared.

We also presented a few numerical examples on the performance of MMSE decision-feedback equalization in DSL transmission at ISDN Basic Access rates with several well-known line codes. Interestingly, the calculated performance is inversely related to the transmission baudrate, except in the case of the simple (N)RZ code, which frequently performs as well as the MS43.

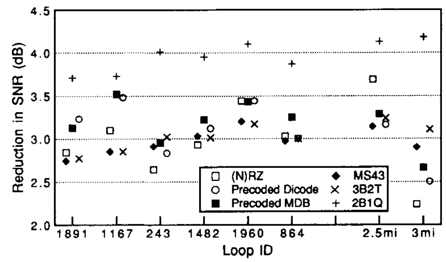

(a)

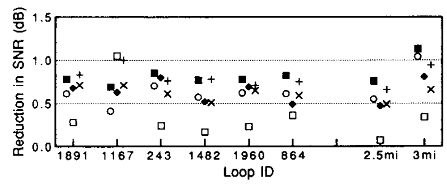

(b)

Fig. 8. Reduction in transmission performance from shortening the DFE. (a) As feedback filter is shortened from of infinite length to 30 taps, at a forward filter length of 8 taps. (b) As forward filter is shortened from 8 taps to 3 taps, at a feedback filter length of 30 taps.

Appendix
MMSE Solution when Both DFE Filters are Infinite in Length

Although in this case it is possible to formulate and solve the MMSE problem in the frequency domain, starting with the time-domain formulation is no less convenient and avoids the introduction of some new notions. Thus, we shall proceed by further developing (9), (10), and (2a). A frequency-domain expression of the solution will surface in the process.

The shift of time origin moves us to a new viewpoint for comprehension and evaluation of the above equations. First, consider the matrix $\boldsymbol{R}_1$. As the forward filter is now (two-sided) infinite, the quantities $\boldsymbol{R}_x, \boldsymbol{H}, \Pi, \boldsymbol{I}, \boldsymbol{K}$, and $\boldsymbol{M}$ are "full-plane" matrices which are (two-sided) infinite in both row and column dimensions. Indexing of their rows and columns can be more conveniently done using both positive and negative integers, with the "center" rows and columns (those corresponding to time zero) indexed by zero. The quantity $\boldsymbol{P}$ is a half-plane matrix, infinite column-wise and semi-infinite (to the right) row-wise. Its negative- and zero-indexed rows are all equal to zero and its positive-indexed rows form an identity matrix. Its leading column corresponds to time zero. For $\underline{\rho}_1$, the vector $\underline{e}_c$ is now infinite and is everywhere zero except for a unity zeroth element. By the upper-triangular nature of $\boldsymbol{K}'\boldsymbol{H}'\boldsymbol{M}$ and Π', the nonzero elements of $\underline{\rho}_1$ are confined to the "anticausal" half.

To obtain the MMSE solution, an immediate problem is the computation of $\boldsymbol{R}_1^{-1}$. (As in Section III, concern over its invertibility will go away as we later consider spectral factorizations. Similar is true for $(\boldsymbol{K}'\boldsymbol{R}_x\boldsymbol{K})^{-1}$ below.) We appeal to the following well-known identity for matrix inversion: $(\boldsymbol{X}+\boldsymbol{YZW})^{-1} = \boldsymbol{X}^{-1} - \boldsymbol{X}^{-1}\boldsymbol{Y}(\boldsymbol{Z}^{-1}+\boldsymbol{W}\boldsymbol{X}^{-1}\boldsymbol{Y})^{-1}\boldsymbol{W}\boldsymbol{X}^{-1}$. Making the identifications that $\boldsymbol{X} = \boldsymbol{K}'\boldsymbol{R}_x\boldsymbol{K}, \boldsymbol{Z} = \sigma_u^2\boldsymbol{I}$, and $\boldsymbol{Y} = \boldsymbol{W}' = \boldsymbol{K}'\boldsymbol{H}'\boldsymbol{M}\Pi'(\boldsymbol{I}-\boldsymbol{PP}')$, we get

$$\boldsymbol{R}_1^{-1} = (\boldsymbol{K}'\boldsymbol{R}_x\boldsymbol{K})^{-1} - \sigma_u^2(\boldsymbol{K}'\boldsymbol{R}_x\boldsymbol{K})^{-1}\boldsymbol{K}'\boldsymbol{H}'\boldsymbol{M}\Pi' \cdot (\boldsymbol{I}-\boldsymbol{PP}')\Phi(\boldsymbol{I}-\boldsymbol{PP}')\Pi\boldsymbol{M}'\boldsymbol{HK}(\boldsymbol{K}'\boldsymbol{R}_x\boldsymbol{K})^{-1} \tag{A.1}$$

where

$$\Phi = [\boldsymbol{I} + \sigma_u^2(\boldsymbol{I}-\boldsymbol{PP}')\Pi\boldsymbol{M}'\boldsymbol{HK}(\boldsymbol{K}'\boldsymbol{R}_x\boldsymbol{K})^{-1} \cdot \boldsymbol{K}'\boldsymbol{H}'\boldsymbol{M}\Pi'(\boldsymbol{I}-\boldsymbol{PP}')]^{-1}. \tag{A.2}$$

Simple algebraic manipulations then lead to

$$\underline{h}_f = \boldsymbol{R}_1^{-1}\underline{\rho}_1 = \sigma_u^2(\boldsymbol{K}'\boldsymbol{R}_x\boldsymbol{K})^{-1}\boldsymbol{K}'\boldsymbol{H}'\boldsymbol{M}\Pi'(\boldsymbol{I}-\boldsymbol{PP}')\Phi\underline{e}_c \tag{A.3}$$

and

$$\sigma_\varepsilon^2 = \sigma_u^2 - \underline{\rho}_1'\boldsymbol{R}_1^{-1}\underline{\rho}_1 = \sigma_u^2\underline{e}_c'\Phi\underline{e}_c. \tag{A.4}$$

Equations (A.2)–(A.4) appear formidable and, at the first sight, it may seem that we have complicated the problem rather than simplfied it. However, the matrix Φ exhibits an interesting structure and, if the noise autocorrelation matrix $\boldsymbol{K}'\boldsymbol{R}_x\boldsymbol{K}$ is Toeplitz or block-Toeplitz, then Φ and the MMSE solution can be evaluated with available techniques.

Consider first the evaluation of Φ. To start, note that, if $\boldsymbol{K}'\boldsymbol{R}_x\boldsymbol{K}$ is (block) Toeplitz, then $(\boldsymbol{K}'\boldsymbol{R}_x\boldsymbol{K})^{-1}$ is also (block) Toeplitz. Thus, since $\Pi\boldsymbol{M}'\boldsymbol{HK}$ is (block) Toeplitz, the factor $\Pi\boldsymbol{M}'\boldsymbol{HK}(\boldsymbol{K}'\boldsymbol{R}_x\boldsymbol{K})^{-1}\boldsymbol{K}'\boldsymbol{H}'\boldsymbol{M}\Pi$ (denoting it by Δ below for short) in (A.2) is a full-plane (block) Toeplitz matrix. Its pre- and postmultiplications by $\boldsymbol{I}-\boldsymbol{PP}'$ simply zero out all elements outside the upper-left "quadrant." Hence Φ^{-1} is the direct sum of a semi-infinite (block) Toeplitz matrix and a semi-infinite diagonal matrix, where only the former enters into the final expressions for the MMSE solution because of the pre- and postmultiplications by $\underline{e}_c$ and $\boldsymbol{I}-\boldsymbol{PP}'$ in (A.3) and (A.4). By its (block) Toeplitz nature, inversion of this semi-infinite matrix can be achieved by way of (matrix) spectral factorization.

To further specify this factorization, we limit our scope by assuming that the sampled noise process x is stationary and let $S_x(\omega)$ denote its power spectrum. Then $\boldsymbol{K}'\boldsymbol{R}_x\boldsymbol{K}$ is indeed Toeplitz and is associated with a power spectrum $\frac{1}{k}\sum_{i=0}^{k-1} S_x(\omega_{mi/k})$ where we have defined $\omega_r \equiv \omega + 2\pi r/T$. A frequency-domain expression of Φ can be obtained by first noting that the quantity $\boldsymbol{HK}(\boldsymbol{K}'\boldsymbol{R}_x\boldsymbol{K})^{-1}\boldsymbol{K}'\boldsymbol{H}'$ has an associated matrix power spectrum as shown at the bottom of the page, where * denotes complex conjugation and $\Theta_p(\omega) = \Theta(\omega)e^{jp\omega T/m}$. Therefore, the quantity $\boldsymbol{M}'\boldsymbol{HK}(\boldsymbol{K}'\boldsymbol{R}_x\boldsymbol{K})^{-1}$ $\boldsymbol{K}'\boldsymbol{H}'\boldsymbol{M}$ is associated with a $k \times k$ matrix power spectrum whose ijth element is given by

$$\frac{1}{m}\sum_{p=0}^{m-1} \cdot \frac{\left[\frac{1}{k}\sum_{q=0}^{k-1}\Theta_{-k+i}\left(\omega_{(mq+p)/k}\right)\right]\left[\frac{1}{k}\sum_{q=0}^{k-1}\Theta_{-k+j}^*\left(\omega_{(mq+p)/k}\right)\right]}{\frac{1}{k}\sum_{q=0}^{k-1} S_x\left(\omega_{(mq+p)/k}\right)}$$

Now, the matrix Π can be viewed as a block Toeplitz matrix with $k \times k$ blocks and associated with a matrix transfer function whose ijth element being $\frac{1}{k}\sum_{q=0}^{k-1} P_{i-j}(\omega_{q/k})$ where $P_p(\omega) = P(\omega)e^{jp\omega T}$. Hence, the matrix power spectrum associated with the quantity Δ is given by $\left[\frac{1}{k}\sum P_{i-j}\right]\left[\frac{1}{km}\sum\frac{\sum\Theta_{-k+i}\sum\Theta_{-k+j}^*}{\sum S_x}\right]\left[\frac{1}{k}\sum P_{i-j}^*\right]'$. Call it $\boldsymbol{W}(\omega)$ for short. Then the matrix power spectrum associated with the upper-left quadrant of Φ^{-1} is given by $\boldsymbol{I}+\sigma_u^2\boldsymbol{W}(\omega)$. Note that $\boldsymbol{W}(\omega)$ reduces to a scalar in some cases, for example, when $k=1$ or when the channel bandwidth is less than $\frac{m}{2kT}$ (so that no aliasing occurs in the DFE forward filter).

Let $\boldsymbol{I}+\sigma_u^2\boldsymbol{W}(\omega)$ be spectral factorized as

$$\boldsymbol{I}+\sigma_u^2\boldsymbol{W}(\omega) = [\boldsymbol{V}'(\omega)]^{-1}\boldsymbol{D}^{-1}[\boldsymbol{V}^*(\omega)]^{-1}, \tag{A.5}$$

where $\boldsymbol{D}$ is a $k \times k$ diagonal matrix and $\boldsymbol{V}(\omega)$ is of minimum phase [20] and has a series expansion whose leading term is lower-triangular with unity diagonal elements. To further relate this to Φ, it is convenient to define a permutation operator $\boldsymbol{J}$ which "reverses the time" for a k-vector sequence. In other words, $\boldsymbol{J}$ is a block antidiagonal matrix with $k \times k$ identity matrices on its antidiagonal. The upper-left quadrant

$$\frac{\left[\frac{1}{k}\sum_{i=0}^{k-1}\Theta_{-k+1}\left(\omega_{mi/k}\right), \frac{1}{k}\sum_{i=0}^{k-1}\Theta_{-k+2}\left(\omega_{mi/k}\right), \cdots, \frac{1}{k}\sum_{i=0}^{k-1}\Theta_{0}\left(\omega_{mi/k}\right)\right]'[\text{same}]^*}{\frac{1}{k}\sum_{i=0}^{k-1} S_x\left(\omega_{mi/k}\right)}$$

of Φ^{-1} is thus turned into the lower-right quadrant in $J\Phi^{-1}J$. Denote this semi-infinite matrix by $\overline{\Phi}^{-1}$. By the summetry of $\Phi^{-1}, \overline{\Phi}^{-1}$ is associated with a matrix power spectrum $I + \sigma_u^2 W'(\omega)$. Thus

$$\overline{\Phi} = \Gamma\Lambda\Gamma' \tag{A.6}$$

where $\Lambda = \mathrm{diag}(D, D, \cdots)$ and Γ is the lower-triangular block Toeplitz matrix associated with $V(\omega)$. Γ has $k \times k$ blocks and unity diagonal elements.

Therefore, from (A.4) we have the MMSE as

$$\sigma_\varepsilon^2 = \sigma_u^2 \sigma_\gamma^2 \tag{A.7}$$

where σ_γ^2 denotes the leading diagonal element in D. From (A.3) we have the MMSE forward filter as

$$F(\omega) = \frac{\sigma_u^2\sigma_\gamma^2}{\frac{1}{k}\sum_{p=0}^{k-1} S_x(\omega_{mp/k})} \cdot \left[\frac{1}{k}\sum \Theta^*_{-k+i}\right]'\left[\frac{1}{k}\sum P^*_{i-j}\right]' \underline{\gamma}^*(\omega) \tag{A.8}$$

where $\underline{\gamma}^*(\omega)$ is the leftmost column of $V^*(\omega)$. $[\frac{1}{k}\sum P^*_{i-j}]$ is a shorthand for the $k \times k$ matrix whose ijth element is given by $\frac{1}{k}\sum_{p=0}^{k-1} P^*_{i-j}(\omega_{p/k})$, and $[\frac{1}{k}\sum \Theta^*_{-k+i}]$ is a shorthand for the k-vector whose ith element is given by $\frac{1}{k}\sum_{p=0}^{k-1}\Theta^*_{-k+i}(\omega_{mp/k})$, with $1 \le i \le k$ and $1 \le j \le k$. For the MMSE feedback filter, we note first that from (A.3) the quantity $\Pi(M'HK\underline{h}_f)$ in (10) corresponds to a transfer function $\sigma_u^2\sigma_\gamma^2 W(\omega)\gamma^*(\omega)$. From (A.5) we get $\sigma_u^2\sigma_\gamma^2 W(\omega)\underline{\gamma}^*(\omega) = \underline{\xi}(\omega) - \sigma_\gamma^2\underline{\gamma}^*(\omega)$ where $\underline{\xi}(\omega)$ is the leftmost column of $[V'(\omega)]^{-1}$. Now, the premultiplication by P' in (10) denotes a projection onto the strictly causal subaxis of time. Hence, we obtain

$$B(\omega) = e^{j\omega T} \cdot \left[[1, e^{-j\omega T}, \cdots, e^{-j(k-1)\omega T}]\left[\frac{1}{k}\sum P_{i-j}\right]^{-1}\underline{\xi}(\omega) - 1\right]. \tag{A.9}$$

An interesting expression exists for the channel-noise power after equalization, i.e., the quantity $\underline{h}_f' K' R_x K \underline{h}_f$. By (A.2), (A.3), and (A.6), it can be expressed as

$$\begin{aligned}\underline{h}_f' K' R_x K \underline{h}_f &= \sigma_u^2 \underline{e}_c' \Phi(\Phi^{-1} - I)\Phi \underline{e}_c \\ &= \sigma_u^2\left(\underline{e}_c'\Phi\underline{e}_c - \underline{e}_c'\Phi^2\underline{e}_c\right) \\ &= \sigma_\varepsilon^2\left[1 - \sigma_\gamma^2 \frac{T}{2\pi}\int_0^{\frac{2\pi}{T}} \underline{\gamma}^{*\prime}(\omega)\,\underline{\gamma}(\omega)\,d\omega\right].\end{aligned} \tag{A.10}$$

Extension of above results to more general conditions can be done in a similar spirit.

ACKNOWLEDGMENT

I thank Prof. J. M. Cioffi of Stanford University for the stimulating discussions during the derivation of the theory for the limiting conditions. I also would like to thank the anonymous reviewers for their comments. One of them also brought [10] to my attention.

REFERENCES

[1] S. U. H. Qureshi, "Adaptive equalization," *Proc. IEEE,* vol. 73, pp. 1349–1387, Sept. 1985.
[2] J. Salz, "Optimum mean-square decision feedback equalization," *Bell Syst. Tech. J.,* vol. 52, pp. 1341–1373, Oct. 1973.
[3] P. Monsen, "Feedback equalization for fading dispersive channels," *IEEE Trans. Inform. Theory,* vol. IT-17, pp. 56–64, Jan. 1971.
[4] C. A. Belfiore and J. H. Park, Jr., "Decision feedback equalization," *Proc. IEEE,* vol. 67, pp. 1143–1156, Aug. 1979.
[5] D. G. Messerschmitt, "Design of a finite impulse response for the Viterbi algorithm and decision-feedback equalizer, *IEEE Int. Conf. Commun. Conf. Rec.,* paper 37D, 1974.
[6] F. D. Waldhauer, "Quantized feedback in an experimental 280 Mb/s digital repeater for coaxial transmission," *IEEE Trans. Commun.,* vol. COM-22, pp. 1–5, Jan. 1974.
[7] P. Monsen, "Theoretical and measured performance of a DFE modem on a fading multipath channel," *IEEE Trans. Commun.,* vol. COM-25, pp. 1144–1153, Oct. 1977.
[8] P. J. van Gerwen, N. A. M. Verhoeckx, and T. A. C. M. Claasen, "Design considerations for a 144 kbit/s digital transmission unit for the local telephone network," *IEEE J. Select. Areas Commun.,* vol. SAC-2, pp. 314–323, Mar. 1984.
[9] P. F. Adams, S. A. Cox, R. B. P. Carpenter, and N. G. Cole, "A long reach digital subscriber loop transceiver," *IEEE Global Telecommun. Conf. Rec.,* 1986, pp. 39–43.
[10] W. F. McGee, "Coding, equalization and feedback of digital cable pair signals," *Canadian Elec. Eng. J.,* vol. 7, no. 1, pp. 3–8, 1982.
[11] J. W. Lechleider, "Digital subscriber line terminals for use with correlated line codes," *IEEE Trans. Commun.,* vol. COM-35, pp. 1029–1036, Oct. 1987.
[12] D. W. Lin, "Minimum mean-squared error echo cancelation and equalization for digital subscriber line transmission: Part I—theory and computation," *IEEE Trans. Commun.,* vol. 38, pp. 31–38, Jan. 1990.
[13] ——, "Minimum mean-squared error echo cancelation and equalization for digital subscriber line transmission: Part II—A simulation study," *IEEE Trans. Commun.,* vol. 38, pp. 39–45, Jan. 1990.
[14] U. Grenander and G. Szego, *Toeplitz Forms and Their Applications.* New York: Chelsea, 1984, 2nd ed.
[15] P. Kabal and S. Pasupathy, "Partial-response signaling," *IEEE Trans. Commun.,* vol. COM-23, pp. 921–934, Sept. 1975.
[16] P. A. Franaszek, "Sequence-state coding for digital transmission," *Bell Syst. Tech. J.,* vol. 47, pp. 143–157, Jan. 1968.
[17] G. L. Cariolaro and G. P. Tronca, "Spectra of block coded digital signals," *IEEE Trans. Commun.,* vol. COM-22, pp. 1555–1564, Oct. 1974.
[18] F. A. Graybill, *Introduction to Matrices with Applications in Statistics.* Belmont, CA: Wadsworth, 1969.
[19] C. R. Rao and S. K. Mitra, *Generalized Inverse of Matrices and Its Applications.* New York: Wiley, 1971.
[20] B. D. O. Anderson and J. B. Morre, *Optimal Filtering.* Englewood Cliffs, NJ: Prentice-Hall, 1979.
[21] J. D. Markel and A. H. Gray, Jr., *Linear Prediction of Speech.* Berlin: Springer-Verlag, 1976. Chapter 6.
[22] J. Makhoul, "Linear prediction: A tutorial review," *Proc. IEEE,* vol. 63, pp. 561–580, Apr. 1975.
[23] A. V. Oppenheim and R. W. Schafer, *Digital Signal Processing.* Englewood Cliffs, NJ: Prentice-Hall, 1975.
[24] J. C. Bellamy, *Digital Telephony.* New York: Wiley, 1982.
[25] A. J. Gibbs and R. Addie, "The covariance of near end crosstalk and its application to PCM system engineering in multipair cable," *IEEE Trans. Commun.,* vol. COM-27, pp. 469–477, Feb. 1979.
[26] Bellcore, "ISDN basic access digital subscriber lines," Tech. Ref. TR-TSY-000393, Issue 1, May 1988.
[27] J. Salz, "On mean-square decision feedback equalization and timing phase," *IEEE Trans. Commun.,* vol. COM-25, pp. 1471–1476, Dec. 1977.

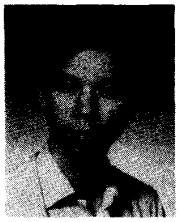

David W. Lin (S'78–M'82–SM'88) received the B.S. degree in 1975 from National Chiao Tung University, Hsinchu, Taiwan, China, and the M.S. and Ph.D. degrees in 1979 and 1981, respectively, from the University of Southern California, Los Angeles, all in electrical engineering.

He joined Bell Laboratories, Holmdel, NJ, in August 1981, and performed research in the areas of digital adaptive filtering and echo cancellation. He transferred to Bellcore in January 1984 and has since worked on digital subscriber line transmission, speech coding, and video coding. In August 1990, he joined the faculty of National Chiao-Tung University as a Professor in the Department of Electrical Engineering and the Center for Telecommunications Research, on leave from Bellcore. His research interest includes various topics in signal processing and digital communication.